MULTI TARGET TRACKING ON AERIAL VIDEOS

Gellért Máttyus, Csaba Benedek and Tamás Szirányi

Distributed Events Analysis (DEVA) Research Group
Computer and Automation Research Institute of the Hungarian Academy of Sciences (MTA SZTAKI)
Budapest, 1111, Kende utca 13-17., Hungary
mattyus@sztaki.hu, bcsaba@sztaki.hu, sziranyi@sztaki.hu
http://web.eee.sztaki.hu

KEY WORDS: Motion Compensation, Motion Detection, Multi Object Tracking, UAV Video

ABSTRACT:

In this paper we propose a new method to detect and track multiple moving targets on image sequences recorded by Unmanned Aerial Vehicles (UAVs). Our approach focuses on challenging urban scenarios, where several object are simultaneously moving in various directions, and we must expect frequent occlusions caused by other moving vehicles or static scene objects such as buildings and bridges. In addition, since the UAVs are flying at relatively low altitude, the 3D-ness of the scene affects strongly the camera motion compensation process, and the independent object motions may be often confused by artifacts of frame registration. Our method enables real time operation, processing 320x240 frames at around 15 fps and 640x480 frames at 5 fps.

1 INTRODUCTION

Nowadays Unmanned Aerial Vehicles (UAVs) are becoming more and more important in military operations (Kumar et al., 2001). Since there is no pilot in such aerial vehicles, they can be sent to missions without endangering human life. The lack of personnel has several other benefits, e.g. reduced weight, the mission length is not a function of pilot fatigue, and the planes can achieve better maneuverability since the human tolerance to acceleration is not a limitation anymore.

Detecting objects of interest is a key task in reconnaissance and surveillance applications and also on the combat field. The moving objects are in most cases relevant, since they are frequently vehicles or persons. The automatic detection of these moving objects can help the operator by giving a caution to them. The tracking of the moving objects can also give useful informations i.e. a vehicle is moving toward the defended camp.

Change detection in video sequences can also reduce the size of the data to be transmitted to the control station. To avoid redundancy, there is no need to transmit the pixels belonging to an unchanged area.

In this paper we introduce a method which deals with the above subtasks. The main steps of the proposed approach are demonstrated in Figure 1:

- (i) video stabilization
- (ii) foreground extraction
- (iii) moving object detection
- (iv) tracking

The first step is the compensation of the camera's ego-motion (Benedek et al., 2009). This can be achieved by warping the frames to a common coordinate system, where the images can be considered still. This step can also provide a better visual information to the operator by avoiding the shaking of the camera. The images in the common coordinate system can be handled by similar algorithms to ones developed for fixed cameras. However, we must consider that ego-motion compensation is not totally accurate, thus efficient filtering of the registration noise is needed. The tracking also needs the world coordinate system, where the position of an object in the image refers to it's real position in the world. The transformation to the world coordinate system needs additional information, i.e. global position, camera parameters.

In the image warped into the common coordinate-system, the motion detection is done by background subtraction. Then we obtain a foreground mask, which shows the moving pixels. The moving objects are blobs on the mask, which can be detected and tracked. Note that foreground detection may contain errors, e.g. some blobs can be split, or only parts of a given moving object are covered by its blob. Therefore, some a priori knowledge is needed about the objects of interest. In aerial videos the size of the objects is a good feature, because it can be easily estimated for several targets such as cars or pedestrian, using the camera parameters (camera altitude, angles, focal length).

In the final step, the detection results from the separate frames are assigned to each other by applying Kalman filtering for the consecutive positions and considering the object histograms. The assigned object positions on the frames yield the track.

2 VIDEO STABILIZATION

The ego-motion compensation is achieved by calculating an optimized homogen linear transform between the frames, and warping the images to a common coordinate system.

The applied image registration and alignment techniques are detailed in (Szeliski, 2006).

The perspective transformation between two images taken of a plane surface can described by the homography matrix $\mathbf{H}$. One point p_0 is transformed to p_1 by the following equation:

$$p_1 = \begin{bmatrix} x_1 \\ y_1 \\ z_1 \end{bmatrix} = \begin{bmatrix} H_{11} & H_{12} & H_{13} \\ H_{21} & H_{22} & H_{33} \\ H_{31} & H_{32} & H_{13} \end{bmatrix} \begin{bmatrix} x_0 \\ y_0 \\ 1 \end{bmatrix} \quad (1)$$

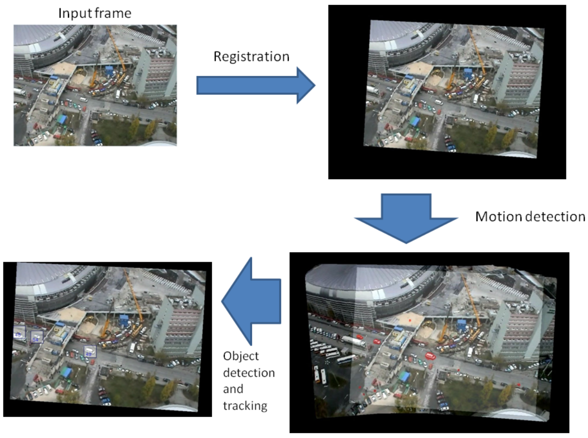

Figure 1: Process overview

The pixel coordinates are:

$$x_{pix} = \frac{x_i}{z_i} \tag{2}$$

$$y_{pix} = \frac{y_i}{z_i} \tag{3}$$

This $\mathbf{H}$ matrix can be calculated for every image pair taken over the same scene, but it will give an accurate transformation only if the scene is a planar surface. This constraint cannot be met in general, but for aerial images it is a good assumption, since the surface of the earth from low altitudes is approximately a plane. This assumption in not met perfectly in the presence of relatively high buildings and considerable relief. In this situations the points emerging from the ground plane surface cause parallax errors in the registration procedure.

In special cases special homography matrices can be used. These are when there is only translation or rotation between two images, or affine transformation. On the considered videos the camera's ego motion is arbitrary, thus we describe the transformation by the most general homography matrix.

To warp one image to the other we need to calculate the $\mathbf{H}$ homography matrix. We mention here two approaches to calculate this matrix:

- Direct (pixel) based
- Feature based

2.1 Direct (pixel) based registration

These approaches define an error metric which shows how much the corresponding pixel values agree after the warping transform. Then the transformation which warps the images with a minimum error is searched, which needs a computationally suitable searching technique.

The advantage of this approach is that it can handle blurred images, when there are no feature points and thus other, feature based, approaches fail (see Section 2.2). On the other hand, this method is mostly suitable for specific transformations, i.e. translation, rotation, but it can hardly handle general homography transformations.

2.2 Feature based registration

The feature based techniques begin with extraction of feature points on the images. These points can be found and aligned on the two image. This yields a points set S on one image which is aligned to point set S' on the other image.

$$S \Rightarrow S'$$

By fitting a transformation to these points the transformation matrix can be estimated.

$$S' = \mathbf{H}S \tag{4}$$

Popular feature point detectors are the Harris corner point detector (Harris and Stephens, 1988), the SIFT detector (Lowe, 2004) and the SURF detector (Bay et al., 2006).

In case of aerial images the transformation cannot be restricted to translation or rotation, thus the more general affine or perspective transformation has to be used. Therefore, we use the feature based method to find the homography matrix of the perspective transformation.

2.3 Feature points

We use the Harris corner detector which is more suitable in man-made environments where corners are abundant. It is also computationally less expensive than the other feature point detectors such as SIFT or SURF. Note that if there are no feature points, like in large homogenous areas, the registration fails.

2.4 Point alignment

Corresponding points are searched on two consecutive frames by the Lucas-Kanade pyramidal optical flow algorithm. This step yields the positions of the feature points on the next image, thus the transformation between the frames can be calculated. The applied optical-flow algorithm assumes small displacement and nearly constant pixel intensity across the consecutive frames. This constraint is fulfilled on the considered videos. The transformation is fitted by RANSAC (Fischler and Bolles, 1981) to the extracted point correspondences to reduce the effect of outliers.

If the transformation between two frames is available, the frames can be warped into a common coordinate-system. The common coordinate system is a periodically chosen reference frame. There is a homography matrix between the two following frames $n, n-1$ $\mathbf{H}_{n,n-1}$, and a homography between the frame and the reference frame $\mathbf{H}_{n,0}$,:

$$\mathbf{H}_{n,0} = \mathbf{H}_{n,n-1}\mathbf{H}_{n-1,n-2}\ldots\mathbf{H}_{2,1}\mathbf{H}_{1,0} \tag{5}$$

The current image is warped into the coordinate-system of the reference image by the Homography matrix $\mathbf{H}$, I_d is the pixel value in the destiny image, I_s is the pixel value in the source image.

$$I_d(x,y) = I_s\left(\frac{H_{11}x + H_{12}y + H_{13}}{H_{31}x + H_{32}y + H_{33}}, \frac{H_{21}x + H_{22}y + H_{23}}{H_{31}x + H_{32}y + H_{33}}\right) \tag{6}$$

The warped image has artifacts, because of the unperfect estimation of the transformation and discretization errors.The homography transformation results in continuous coordinate values which

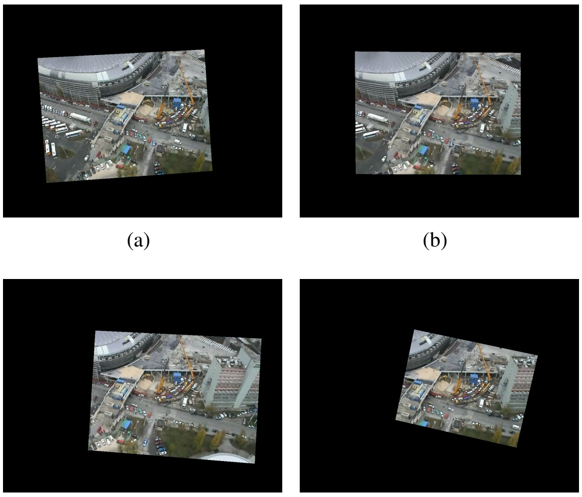

(a) (b) (c) (d)

Figure 2: Warped frames

should be discretized into pixel positions, which may be relevant in strong perspective cases, when a given source pixel is warped to several pixels of the output image. This reduces the effective resolution of the image.

3 FOREGROUND EXTRACTION

The image registration yields an image that looks like a window in a global image (see Figure 2). If the registration is optimal only the pixels belonging to a moving object are changing, though this cannot be fully achieved due to image registration and parallax errors.

Working on the considered videos, these errors are typically located along the edges and their expansion is narrow (a few pixels).

3.1 Background model

The background image is synthesized and updated in the common coordinate system, calculating the pixel-by-pixel running average and variance of the consecutive warped video frames. Note that the widely used Mixture of Gaussians (MOG) approach (Stauffer and Grimson, 1999) cannot be adapted to our case, since due to the fast camera motion we can often observe only a few samples (less than 10) for each surface point, which is not enough to describe the distribution by MOG.

We calculate the mean value $\bar{x}_n$, and the variance σ_n^2 for every pixel on-line:

$$\bar{x}_n = (1-\alpha)\bar{x}_{n-1} + \alpha x_n \tag{7}$$

where α is a constant that gives the refresh rate.

$$\sigma_n^2 = (1-\alpha)\sigma_{n-1}^2 + \alpha(x_n - \bar{x}_n)(x_n - \bar{x}_{n-1}) \tag{8}$$

3.2 Foreground detection

The pixels of the actual frame are classified either as foreground or background based on the normalized Euclidean distance from the background pixel values in the CIE L*u*v* color space. This is the Mahalanobis-distance for diagonal covariance matrix.

$$d(p_n) = \sqrt{\sum_{i=1}^{3} \frac{(p_{n,i} - \bar{p}_{n-1,i})^2}{\sigma_{n-1,i}^2}} \tag{9}$$

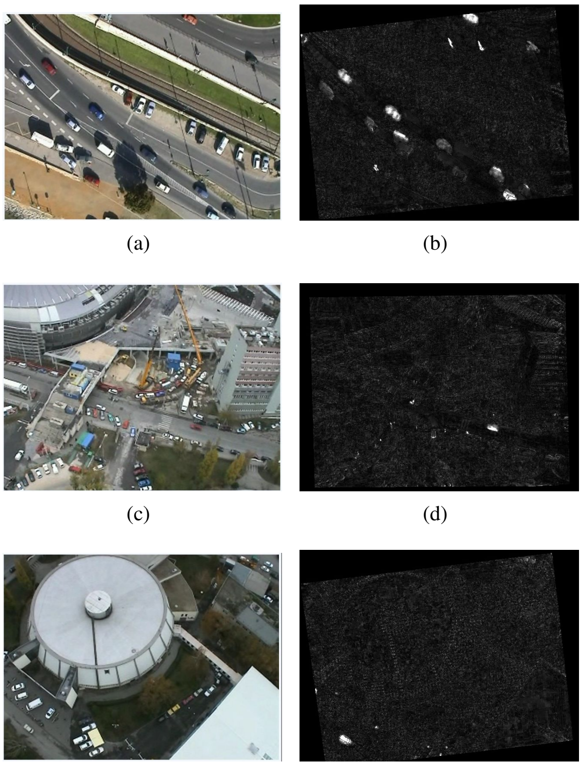

(a) (b) (c) (d) (e) (f)

Figure 3: Results of background subtraction

This yields a distance image, which is noisy as one can see on Figure 3. This noisy image is filtered by a special Difference of Gaussians filter, applying Gaussian blur and threshold. The blurring spreads the narrow pixel errors, thus the concerning values in the difference image drop below the threshold level. The moving objects correspond to blobs on the foreground mask, though the mask of an object can be split and incomplete. Figure 4 shows the foreground mask marked by red color on the image.

4 MOVING OBJECT DETECTION

The foreground detection yields a binary mask on which the moving objects, e.g. cars and pedestrians are blobs. These blobs can be noisy, split, etc., and there can be false detected blobs which do not belong to moving objects. So in general the blob detection is under-constrained. By using a priori knowledge the blob detection can be restricted to special blobs, i.e. by shape or size.

We propose a fast object detection algorithm which is based on the foreground mask; meanwhile it considers split and incomplete object blobs. The input is the size of a car. The size of the cars can be precisely defined. If we know the altitude, the angles (raw, pitch) and the focus length of the camera(the airborne vehicles have an inertial navigation system which can provide these parameters) the size of the car can be approximately calculated by assuming that it is moving on the ground. On the videos we have tested these parameters are unknown, thus we have estimated the size of the cars manually.

The initial step of the object detector algorithm divides the mask image to disjunctive rectangles with size $x \times x$, where x is the size of the car in pixels, and the foreground covering ratio is calculated for each rectangle. The rectangles containing foreground pixels above a threshold are kept as object candidates (OC).

Next, the OC-s are shifted and/or merged by an iterative algorithm. An OC is shifted by mean-shift based on the binary mask

(a)

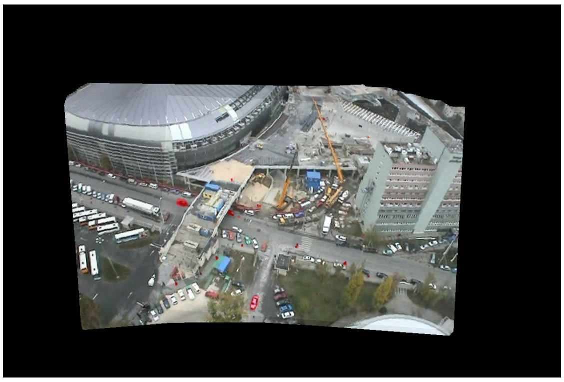

(b)

Figure 4: Foreground detection. Moving objects are marked by red color on the mosaic image.

values. This shift moves the OC rectangles toward the dense foreground pixel regions. Thereafter, these two OCs are merged, if in the shifted positions their overlapping area is above a threshold. The meanshifting and merging steps are repeated several times till convergence.

At the end the OCs are located around areas containing large number of foreground pixels. Since the binary meanshifting and intersection calculations are very simple operations the detection algorithm is significantly quicker than similar approaches, e.g. the color and texture based methods proposed in (Yu et al., 2008). But since it is based only on the foreground mask, it can fail in cases when the foreground mask has errors, e.g. the large objects e.g. buses, can be detected as more cars if their silhouette is split.

Also the pedestrians can cause false positive errors, if more moving pedestrians are close, because in this case their foreground blob's size is close to the size of a car. The steps of the algorithm can be followed in Fig. 4.

5 TRACKING

The object detection is processed for each frame independently. Thus these detections have to be assigned across the frames to yield the tracks of the objects. The difficulty is that in general the number of object detections for consecutive frames can vary even in the case of perfect detection, i.e. objects enter and leave the scene, objects are occluded by buildings or bridges. To handle the disappearing and later reappearing objects Kalman filtering is used.

The steps of tracking are shown in figure 6.

The steps of the detection:

1. calculate the foreground pixels n_{fore} in the $x \times x$ sized rectangles R_i
2. if $n_{fore} > \beta A_{(R_i)}$ (where A means the area of the rectangle and β is the threshold parameter) R_i will be an object candidate and the "mass center" is calculated for R_i
3. Find the n closest neighbors N_j for every object candidate R_i. I used $n = 4$
4. Calculate the areas A_{ij} of the cuts between the neighbors and the object candidate $A_{ij} = A(R_i \cap N_j)$
5. if $A_{ij} > \xi$ where ξ is a threshold parameter the OCs $R_i R_j$ are merged, this means that the OC with less foreground pixels is deleted and the size of the other is increased.
6. The position of the object candidates is modified by mean shifting it m times. m is a parameter, which is different in the iteration steps. In the first iterations it is low (2-3), later it is increased to 4-5. This accelerates the algorithm, since in the first iterations when the number of OCs is high less mean shifting is needed.
7. The steps 4 – 6 are repeated till convergence with different ξ and m parameters. Practically the convergence can be achieved by repeating the steps several times.
8. The remaining OC rectangles are the objects, the 1 dimensional histogram is calculated for every color channel in the HSV color space for the objects.

Figure 5: Moving object detection

5.1 Kalman filter

The Kalman filter is an efficient tool for filtering a noisy dynamic system. It predicts the new states of the system and then corrects it by the measurements.

In tracking we do not have information about the control of the motion, therefore the acceleration is assumed to be zero, and the change in velocity is modeled by the process noise. Consequently, we do not include the acceleration in the process equation, and the effect of the acceleration noise is described by the velocity noise. The motion can be described by the following equations:

$$\vec{x}_k = \begin{bmatrix} x_k \\ \dot{x}_k \end{bmatrix} = \begin{bmatrix} 1 & 1 \\ 0 & 1 \end{bmatrix} \begin{bmatrix} x_{k-1} \\ \dot{x}_{k-1} \end{bmatrix} + w_{k-1} \quad (10)$$

$$z_k = [1\ 0]\, \vec{x}_k + v_k \quad (11)$$

Where x_k is the position coordinate in one direction, z_k is the measured position, w_{k-1} is the process noise, v_k is the measurement noise.

5.2 Assignment

On each current frame the k detected objects have to be assigned to n tracked objects from the previous frames. If $n = k$, this can be done in $n!$ ways. The Hungarian method solves this in $O(n^3)$ running time. We solve the assignment problem with a greedy algorithm, which is computationally simple and gives good result in most cases. The cases when the greedy algorithm fail can be neglected, since they last only a few frames, and on a long term the Kalman filtering corrects these errors.

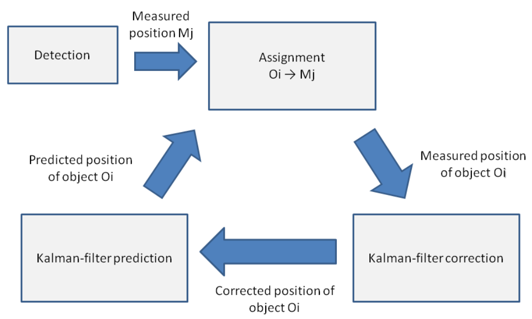

Figure 6: The steps of object assignment with Kalman-filtering

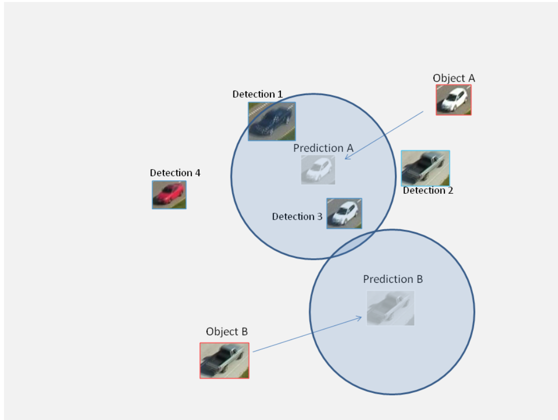

Figure 7: Object assignment

We construct a $n \times k$ score matrix, S, whose elements are calculated based on the euclidean distance of the predicted and detected positions and the object's color histogram. The elements of the matrix are fitness values which describe how good the objects from the previous frames match the objects detected on the current frame.

$$S_{ij} = \vartheta \frac{1}{d_{pos(O_i,D_j)}} + (1-\vartheta) d_{hist(O_i,D_j)} \tag{12}$$

where d_{pos} is the euclidean distance of the positions, d_{hist} is the histogram similarity and ϑ is a weight value.

$$d_{pos(O_i,D_j)} = \sqrt{(\hat{p}^-_{i,x} - p_{j,x})^2 + (\hat{p}^-_{i,y} - p_{j,y})^2} \tag{13}$$

$\hat{p}^-_i$ is the predicted position of object O_i, p_j is the position of detected object O_j.

The steps of the score table S_{ij} calculation for every i, j pair:

1. Calculate the distance d_{pos} of the predicted position $\hat{p}^-_i$ of object O_i and the position p_j of the detected object D_j.
2. if $d_{pos\ i,j} > \zeta$, $S_{ij} = 0$ and terminate. ζ is a threshold parameter.
3. if $d_{pos\ i,j} \leq \zeta$ calculate S_{ij} according to (12)

If the number of detected objects is equal or greater than the number of tracked objects from the previous frames, the assignment is done forward, this means that the tracked objects are assigned to the detected ones.

The steps of forward assignment:

1. i=1
2. for O_i find max m_i in $S_{i1...k}$, $m_i = S_{ij}$
3. if $m_i > \zeta$, assign D_j to O_i, set the column $S_{1...nj} = 0$
4. $i = i + 1$, go to step 2 until $i \leq n$
5. set the not assigned objects O_{na} to passive, $O_{na} \rightarrow$ passive
6. create new objects O_{new} for the detections which are not assigned to an object D_{na}, and assign these new objects to them. $O_{new} \rightarrow D_{na}$

The objects which are passive for more than $N_{passive}$ time are deleted.

If the number of detected objects is less than the number of tracked objects from the previous frames, the assignment is done backward, this means that the detected objects are assigned to the tracked ones. Distinguishing between the two assignments is needed because the algorithm is greedy, thus the first objects in the order have priority.

Assignment backward:

1. j=1
2. for D_j find max m_j in $S_{1...nj}$, $m_j = S_{ij}$
3. if $m_j > \zeta$, assign O_i to D_j, set the row $S_{i1...k} = 0$
4. $j = j + 1$, go to step 2 until $j \leq k$
5. set the not assigned objects O_{na} to passive, $O_{na} \rightarrow$ passive
6. create new objects O_{new} for the detections which are not assigned to an object D_{na}, and assign these new objects to them. $O_{new} \rightarrow D_{na}$

During the assignment process:

- Objects are assigned to detections.
- New objects are created and assigned to detections.
- Objects are set to passive. (no detections are assigned to them)
- Objects are deleted.

The figure 7 shows an assignment. A detection is assigned to an object only if it is close enough (this is given by the threshold parameter ζ) to the predicted position of the object. Object A is assigned to detection "3", Object B is not assigned to a detection thus it is set to passive. For the detections 1, 2, 4 new objects are created.

6 RESULTS AND CONCLUSION

The algorithm was tested on various videos, taken in rural, urban and suburban environment from plane and balloon. We evaluate the tracking in a qualitative way.

On the videos which contained corner points over all the image, the registration was accurate, therefore the tracking was also accurate. The videos which lacked corner points could not been registered accurately therefore the algorithm failed.

In the urban environment the algorithm was accurate in weak and middle traffic. Also in the presence of a bridge which occluded the cars.

The dense traffic caused errors, because in this case the algorithm can hardly distinguish between the background and the moving vehicles.

The algorithm was implemented in OpenCV 2.0. The program was tested on an Intel Core i7, 2.67 GHz processor. The execution time per frame, for a 640×480 video was about 250 ms.

One of the most important input is the relative size of the car in pixels. The blob detection on the foreground mask highly depends on this. It has to be considered that the size of the cars varies by the pixel position on the image if the camera view is not vertical. The proposed algorithm calculates with a fixed car size along all the image, thus in horizontal camera views it can fail. This could be handled by a size correction based on the camera's view angle and altitude.

The refresh rate for the foreground detection is also crucial. The ideal value depends on the frame rate, the ego-motion speed of the camera and the speed of the objects. The value was set in an experimental way.

The proposed algorithm is well suited for real-time application, because the computational complex is kept low. The proposed detection algorithm can be used in more complex, e.g. color based object detection as a pre filtering step to reduce the needed computations.

Figure 8(a) and 8(b) show the track results for urban environment containing a bridge that occludes the cars. The whole image is the mean value of the background, the brighter part is the current frame, the rectangles are the objects with their IDs, the colored dots are the tracks.

ACKNOWLEDGEMENT

This work was supported by the Hungarian Research Fund (OTKA 76159).

REFERENCES

Bay, H., Tuytelaars, T. and Gool, L. V., 2006. SURF: Speeded up robust features. In: European Conference on Computer Vision, Graz Austria.

Benedek, C., Szirányi, T., Kato, Z. and Zerubia, J., 2009. Detection of object motion regions in aerial image pairs with a multi-layer Markovian model. IEEE Trans. on Image Processing 18(10), pp. 2303–2315.

Fischler, M. and Bolles, R., 1981. Random sample consensus: A paradigm for model fitting with applications to image analysis and automated cartography. Communications of the ACM 24, pp. 381–395.

Harris, C. and Stephens, M., 1988. A combined corner and edge detector. In: Alvey Vision Conference, pp. 147–152.

Kumar, R., Sawhney, R. H., Samarasekera, S., Hsu, S., Tao, H., Guo, Y., Hanna, K., Pope, A., Wildes, R., Hirvonen, D., Hansen, M. and Burt, P., 2001. Aerial video surveillance and exploitation. In: Proceeding of the IEEE, Vol. 8, pp. 1518–1539.

Lowe, D. G., 2004. Distinctive image features from scale-invariant keypoints. International Journal of Computer Vision 60(2), pp. 91–110.

Szeliski, R., 2006. Image alignment and stitching: a tutorial. Found. Trends. Comput. Graph. Vis. 2(1), pp. 1–104.

Yu, W., Yu, X., Zhang, P. and Zhou, J., 2008. A New Framework of Moving Target Detection and Tracking for UAV Video Application. ISPRS Congress Beijing, Commission III, Working Group III/5 XXXVII(1), pp. 609–614.

(a)

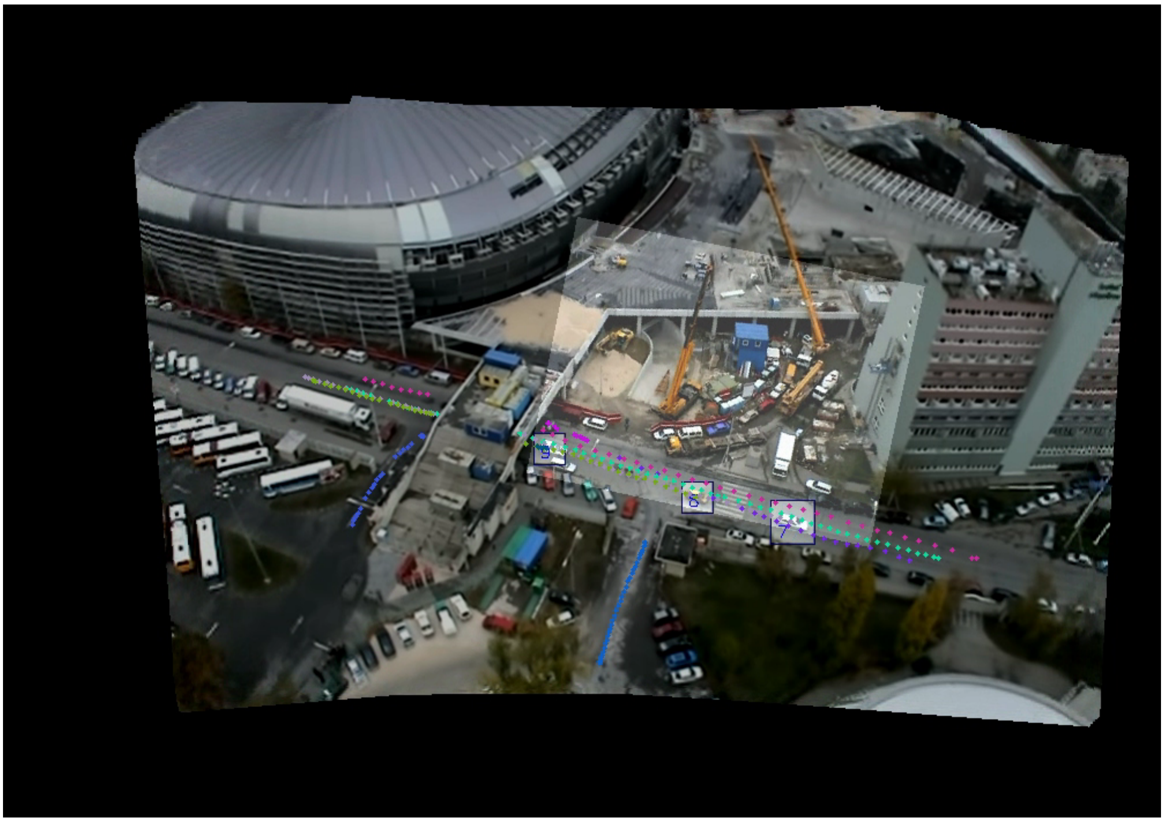

(b)

Figure 8: Track results. The current frame is the brighter region, the objects are marked with rectangles and IDs, the colored dots are the tracks of different cars.